FEBS Letters 588 (2014) 4398–4403

journal homepage: www.FEBSLetters.org

Sites and functional consequence of VDAC–alkylphenol anesthetic interactions

Brian P. Weiser [a,b], Weiming Bu [a], David Wong [c], Roderic G. Eckenhoff [a,*]

[a] Department of Anesthesiology and Critical Care, University of Pennsylvania Perelman School of Medicine, Philadelphia, PA 19104, United States
[b] Department of Pharmacology, University of Pennsylvania Perelman School of Medicine, Philadelphia, PA 19104, United States
[c] Drexel University College of Medicine, Philadelphia, PA 19129, United States

ARTICLE INFO

Article history:
Received 14 August 2014
Revised 10 September 2014
Accepted 10 October 2014
Available online 18 October 2014

Edited by Maurice Montal

Keywords:
Voltage-dependent anion channel
Propofol
Azi-propofol
Photolabeling

ABSTRACT

General anesthetics have previously been shown to bind mitochondrial VDAC. Here, using a photoactive analog of the anesthetic propofol, we determined that alkylphenol anesthetics bind to Gly56 and Val184 on rat VDAC1. By reconstituting rat VDAC into planar bilayers, we determined that propofol potentiates VDAC gating with asymmetry at the voltage polarities; in contrast, propofol does not affect the conductance of open VDAC. Additional experiments showed that propofol also does not affect gramicidin A properties that are sensitive to lipid bilayer mechanics. Together, this suggests propofol affects VDAC function through direct protein binding, likely at the lipid-exposed channel surface, and that gating can be modulated by ligand binding to the distal ends of VDAC β-strands where Gly56 and Val184 are located.

1. Introduction

The mitochondrial voltage-dependent anion channel (VDAC) is a β-barrel protein in the mitochondrial outer membrane. Ions and small metabolites diffuse through the open channel between the cytosol and mitochondrial intermembrane space. The channel remains open under low voltage and has twofold selectivity for anions relative to cations. However, as the transmembrane potential increases to 30–40 mV, VDAC begins to change conformations to various "closed" states. VDAC closure (also referred to as "gating") is characterized by a decrease in channel conductance and a reversal in ion selectivity [1].

The functional properties of VDAC proteins are remarkably conserved across eukaryotic species. However, VDAC function can be affected by membrane composition [2,3], pH [4,5], specific pore block [6], and the small molecule erastin [7]. A number of general anesthetics have also been identified as VDAC ligands, with binding determined by photolabeling with anesthetic analogs [8–23]. These ligands bind VDAC from amphibians, insects, fish, and mammals [8]. While these lipophilic compounds often bind integral membrane proteins after partitioning into membranes, anesthetic binding to VDAC is generally saturable or specific [8]; however, any direct functional relevance of anesthetic–VDAC binding has not been identified.

In previous work, we determined that the anesthetic photolabel *meta*-azi-propofol (AziP*m*), an analog of the clinically used compound propofol (Fig. 1A), binds neuronal VDAC in vivo in *Xenopus laevis* tadpoles [22]. We then determined that AziP*m* binding to VDAC is inhibited by propofol, suggesting conserved binding of the alkylphenols to some saturable VDAC site(s) [22]. To further investigate alkylphenol–VDAC interactions, specifically the binding sites and functional consequences, we transitioned our experiments here to mammalian systems.

2. Materials and methods

2.1. Materials

Propofol (2,6-diisopropylphenol) was from Sigma–Aldrich, and AziP*m* was synthesized according to published methods [24]. AziP*m* was tritiated by Ambios Labs (Newington, CT) and its application has been reported previously [22]. Electrophoresis apparatuses and gels were from Bio-Rad, and DOPC and DOPE were from Avanti Polar Lipids, Inc. (Alabaster, AL). Gramicidin A was a generous gift of O.S. Andersen, Cornell University Medical College. Instrumentation for scintillation counting and UV–Vis spectroscopy are described elsewhere [22].

* Corresponding author at: 3620 Hamilton Walk, Philadelphia, PA 19104, United States. Fax: +1 215 349 5078.
E-mail address: roderic.eckenhoff@uphs.upenn.edu (R.G. Eckenhoff).

http://dx.doi.org/10.1016/j.febslet.2014.10.009

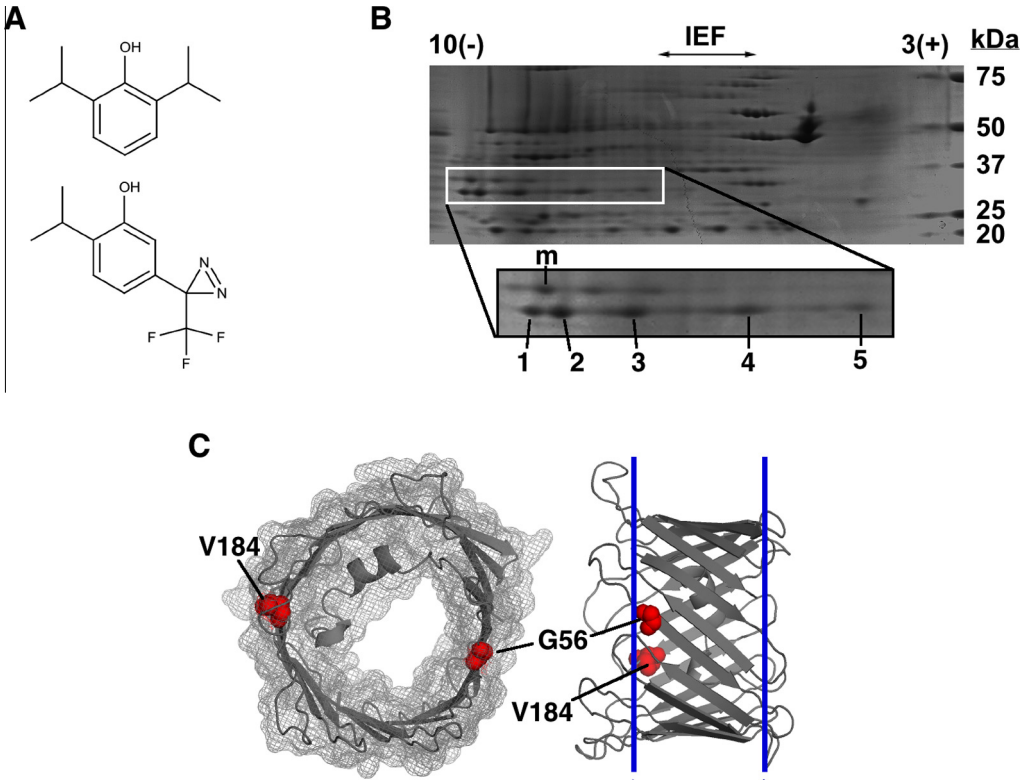

Fig. 1. (A) Propofol (*top*) and AziP*m* (*bottom*) (B) IEF/SDS–PAGE gel of rat brain mitochondria. Spots 1–5 primarily contain VDAC isoforms, and spot "m" contains malate dehydrogenase 2. (C) The location of VDAC1 residues Gly56 and Val184, which are photolabeled by AziP*m*, are indicated in red spheres on the crystal structure of recombinant rat VDAC. (*Left*), the protein surface is shown in mesh, and the view through the barrel is from the cytosolic side. (*Right*), the blue lines indicate the predicted hydrophobic–hydrophilic interface of membrane lipids. Here, the cytosolic side is on the left.

2.2. Brain mitochondria purification

Female Sprague Dawley rats were anesthetized with isoflurane before decapitation. The brains were homogenized in ice-cold isolation buffer (0.32 M sucrose, 5 mM Tris, pH 7.4) supplemented with protease inhibitors, and purified mitochondria were isolated as described without detergents [25]. Aliquots of mitochondria (>5 mg/ml) were frozen in isolation buffer until use.

2.3. IEF/SDS–PAGE

Mitochondria were pelleted, and after removing the isolation buffer, pellets were washed twice with ice-cold 2 mM Tris, pH 7.4. After pelleting again, 150 μg of protein was dissolved in 125 μl of IEF/SDS–PAGE buffer (7 M urea, 2 M thiourea, 20 mM DTT, 4% CHAPS, and 0.2% carrier ampholytes). Isoelectric focusing and SDS–PAGE proceeded according to the manufacturer's instructions using 7 cm IPG strips and 4–15% precast SDS–PAGE gels.

2.4. VDAC identification and LC–MS/MS

Mitochondrial protein was separated by IEF/SDS–PAGE then stained with Coomassie G-250. Protein spots that were candidates for containing VDAC were identified based on molecular weight and isoelectric point. These were excised for LC–MS/MS. Cysteines were alkylated, and after trypsin digestion, samples were injected into a nanoLC column with online electrospray into a Thermo LTQ linear ion trap. XCalibur acquired raw data, and Sequest searched b and y ions. For protein identifications, a database was downloaded from www.uniprot.org with the search term "rattus norvegicus". Search parameters were 1 amu parent ion tolerance, 1 amu fragment ion tolerance, full tryptic digest, one missed cleavage, variable methionine oxidation, and fixed cysteine carboxyamidomethylation. Filter parameters were Xcorr scores (+1 ion) 1.5, (+2 ion) 2.0, (+3 ion) 2.5, deltaCn 0.08, peptide probability >0.05, and two unique peptides.

2.5. Mitochondria photolabeling

Mitochondria were diluted to 1 mg/ml in isolation buffer before adding ligand(s). Samples were incubated at room temperature in the dark for 10 min before photolabeling in a quartz cuvette (pathlength 1 mm) for 15 min with a lamp described elsewhere [22]. After photolabeling, mitochondria were pelleted and washed with ice-cold isolation buffer, pelleted again, then washed twice with 2 mM Tris, pH 7.4. Subsequently, the pellet was dissolved in IEF/SDS–PAGE buffer for two-dimensional electrophoresis.

2.6. Scintillation counting of VDAC spots

After IEF/SDS–PAGE of mitochondrial protein photolabeled with [^{3}H]AziP*m*, gels were Coomassie stained and scanned, and spot intensity was quantified as previously described [22]. VDAC protein spots were then excised, dissolved in H_2O_2, and scintillation counted. Scintillation counts were normalized to spot intensity (i.e., protein abundance) for quantitative analyses.

2.7. Identification of AziPm binding sites

Mitochondria photolabeled with AziP*m* were separated with IEF/SDS–PAGE, the gels were stained, and protein spots were excised and processed for LC–MS/MS as above after either trypsin or chymotrypsin digestion. After LC–MS/MS, the spectra were searched against rat sequences of VDAC1, VDAC2, VDAC3, and

malate dehydrogenase 2. The search parameters and filters described above were used along with a maximum of three post-translational modifications per peptide and a variable AziP*m* modification (+216.08 Da) on any residue. To sequence the N-terminus of VDAC1, however, a specific search for alanine acetylation [26] with partial tryptic digest was required. This procedure confirmed that the N-terminal methionine of VDAC1 is removed during protein maturation in vivo, and also that the second coded residue (alanine) is acetylated [26]; however, we included the coded methionine (Met1) in the numbering of amino acids. For protein sequencing, only the highest scoring peptide assignment for each spectrum was considered, and spectra of peptides containing AziP*m* adducts were manually confirmed.

2.8. Structural analyses

For structural analyses of rat VDAC1, we used PDB code 3EMN, which represents a crystal structure of recombinant rat VDAC refolded from inclusion bodies [27]. This was oriented in a hypothetical membrane with the PPM server of Orientation of Proteins in the Membrane [28], and PyMOL was used for generating structural images [29]. In addition to the 3EMN structure, we referenced a proposed, alternatively-folded VDAC protein with a structural topology that was deduced from experimental studies and has been described elsewhere [30–32]. This protein is proposed to contain an integral transmembrane helix and 13 β-strands [30–32]; however, a high-resolution structure of VDAC that is folded in this manner is not available.

2.9. Reconstitution of VDAC into planar lipid bilayers

Frozen mitochondrial membranes from rat liver were kindly provided by Marco Colombini (University of Maryland, College Park). VDAC was isolated from the membranes by the standard method [33] and purified on a 2:1 hydroxyapatite:celite column following a previously described protocol [34]. Purified VDAC was stored at ~0.2 mg/ml in 10 mM Tris, pH 7.0, 50 mM KCl, 1 mM EDTA, 2.5% Triton X-100, and 15% DMSO at −80 °C.

Planar lipid bilayers were formed from a lipid mixture of 1:1 DOPC:DOPE in pentane from two opposed preformed lipid monolayers as described previously [2,5]. Channel reconstitution was achieved by adding 0.1–0.2 μl of purified VDAC to the ~1.2 ml aqueous solution of 1 M KCl buffered with 5 mM Hepes, pH 7.4, in the *cis* compartment while stirring.

2.10. Electrophysiological recordings of VDAC

All electrophysiology experiments were performed essentially as described [2,5]. Membrane potential was maintained by Ag/AgCl electrodes with 3 M KCl and 15% agarose bridges. Potential was defined as positive when it is greater on the *cis* side, i.e. the side of VDAC addition. An Axopatch 200B amplifier (Axon Instruments, Inc., Foster City, CA) was used in voltage clamp-mode. Single-channel currents were filtered by the amplifier low-pass Bessel filter at 10 kHz. Data were acquired with a Digidata 1440A board (Axon Instruments, Inc.) at a sampling frequency of 50 kHz for single-channel recordings, which were analyzed with pClamp 10.2 software (Axon Instruments, Inc.).

For multichannel experiments, a symmetrical 5 mHz triangular voltage wave with amplitude ±60 mV was applied with a Hewlett Packard 33120A waveform generator [2,5], and data was saved with a 1 Hz sampling frequency. Current responses to 5–10 periods of triangular voltage waves were recorded. For subsequent analyses, the parts of the wave in which VDAC re-opens (i.e., −60 mV to +10 mV, and +60 to −10 mV) were used. Relative multichannel conductance and open probability plots were calculated based on a previously described approach to gating analysis [2,5]. The gating parameters V_0 and n were calculated from the open probability plots as extensively discussed elsewhere [2,5,35,36].

After collecting control data (0 μM propofol), both in single and multichannel experiments, propofol diluted in 1 M KCl, 5 mM Hepes, pH 7.4, was then added to the bath in both the *trans* and *cis* compartments while stirring, and measurements were again collected. After each experiment, the *cis* and *trans* aqueous solutions were collected and the volumes were measured to determine exact propofol concentrations, which were then confirmed with UV spectroscopy.

2.11. Gramicidin A experiments

Planar bilayers of 1:1 DOPC:DOPE were formed as described above in 1 M KCl with 10 mM Hepes, pH 7.2. Gramicidin A from 10^{-9} M ethanol stock solution was added to both aqueous compartments at the amount sufficient to give a single channel activity (~1 μl). For gramicidin A channel lifetime and conductance, the records were digitally filtered at 2 Hz using Bessel algorithm and analyzed using Clampfit 10.2 software as described previously [2]. After control recordings were obtained, propofol dissolved in 1 M KCl and 10 mM Hepes, pH 7.4, was added in increasing concentrations to both compartments. Mean channel conductance was calculated from Gaussian fits to current amplitude histograms, and channel lifetimes were calculated from fits to logarithmic single exponents of at least 250 channel events [2].

3. Results and discussion

To confirm alkylphenol anesthetic binding to mammalian VDAC, we first enriched and identified VDAC protein. We purified rat brain mitochondria then separated the protein with IEF/SDS–PAGE. Initially guided by protein molecular weight and isoelectric point, and subsequently confirmed with LC–MS/MS, we identified five spots that contained VDAC as the major component (Fig. 1B). Although there are only three mammalian VDAC isoforms, each can be post-translationally modified [37], which can alter protein migration during isoelectric focusing. 64–91% of total spectra per spot were assigned to VDAC (Table S1), and each spot contained multiple isoforms.

With VDAC identified, we then photolabeled mitochondria with 10 μM [^{3}H]AziP*m* ±100 μM propofol, again separated the protein with IEF/SDS–PAGE, and dissolved the VDAC gel spots in H_2O_2. Scintillation counting of the VDAC spots after [^{3}H]AziP*m* photolabeling revealed cpm significantly above background (>4-fold each spot), with no selectivity for any spot after normalizing for protein mass. After confirming that [^{3}H]AziP*m* did not bind to the major contaminant in the spots (malate dehydrogenase 2), we determined that 100 μM propofol decreased 10 μM [^{3}H]AziP*m* binding to VDAC by approximately 30%. This is in reasonable agreement with the ~50% displacement of 4 μM [^{3}H]AziP*m* from *X. laevis* VDAC by 400 μM propofol [22].

To identify alkylphenol site(s) on mammalian VDAC, we photolabeled mitochondria with 10 μM (non-radioactive) AziP*m* and sequenced VDAC with LC–MS/MS. Residues photolabeled by AziP*m* were identified by searching VDAC peptides for a 216 Da modification, which corresponds to the mass adduct of photo-reacted AziP*m* [8]. With trypsin digest, we identified Gly56 on VDAC1 as photolabeled in all five spots. To increase sequence coverage, we also digested the most intense spot (spot 2) with chymotrypsin; Val184 on VDAC1 and the homologous residue on VDAC2 (Val196) were identified as photolabeled (Figs. 1C, S1 and S2).

Combining trypsin and chymotrypsin digestions, and combining the five spots, we sequenced 95.7% of VDAC1, 51.9% of VDAC2, and 41.3% of VDAC3 (Fig. S1). Detection with LC–MS/MS is dependent on protein abundance in the samples, which contributed to the variability in sequence coverage, as relative spectra counts for VDAC1:VDAC2:VDAC3 were approximately 10:3:1. Relative abundance may have also contributed to the lack of identified adducts on VDAC3 and a site on VDAC2. The photolabeled glycine and valine of VDAC1 are conserved in all three isoforms, which each share ~70% sequence identity, and are believed to adopt identical folds [38–40]; therefore, alkylphenol binding to these residues on all isoforms remains possible and perhaps likely.

To investigate the locations of the residues that alkylphenols bind, we first used the crystal structure of recombinant mouse and rat VDAC1 (PDB code 3EMN) [27]. We oriented this VDAC structure in a hypothetical membrane to calculate the hydrophobic boundaries of the protein [28]. Both residues were on the cytosolic half of the protein within the predicted bilayer [41], with Gly56 and Val184 at the periphery of β-strands 3 and 12, respectively. The backbone α carbons of Gly56 and Val184 were 3.2 and 2.3 Å, respectively, from the predicted hydrophobic–hydrophilic interface of the protein (Fig. 1C). The membrane depths of these residues are consistent with the predicted distribution of propofol in a bilayer, i.e. at the interface of lipid phospho-head groups and acyl chains [42]. The topology of an alternatively-folded VDAC1 has also been proposed [30–32], and interestingly, this model also places Gly56 and Val184 at the hydrophobic–hydrophilic interface. However, in contrast to the crystal structure, the residues in this model are placed near the membrane surface of opposite leaflets. Regardless, these binding sites should be readily accessible to free ligand dissolved in lipid, assuming that propofol binds the VDAC residues at the lipid-facing channel surface and not inside the pore.

After demonstrating conserved binding of the alkylphenol anesthetics to rat VDAC, we tested whether the clinical compound propofol affects its basic electrophysiological properties. For these experiments, we used native VDAC isolated from rat liver mitochondria, which also contains a mixture of the three VDAC isoforms. We first measured the conductance of open VDAC reconstituted in a planar bilayer of 1:1 DOPC:DOPE (Fig. 2A). The measured single channel conductance of ~4 nS in a bath of 1 M KCl, pH 7.4, is in agreement with previously published values [1]. Addition of propofol (1–18 μM) to the bath did not affect open channel conductance, further suggesting that it is unlikely propofol binds inside the open channel lumen (Figs. 2A, S3 and Table S2).

We therefore tested whether propofol affects the most characteristic VDAC property, its voltage gating. For these experiments, we used identical lipid and bath conditions as before, but reconstituted multiple channels into the planar membrane and applied a slow symmetrical triangular voltage wave with amplitude ±60 mV [2,5,36,43]. At clinically relevant concentrations (1–10 μM), propofol concentration-dependently promoted VDAC closure at negative voltages (Fig. 2B). Because VDAC inserts unidirec-

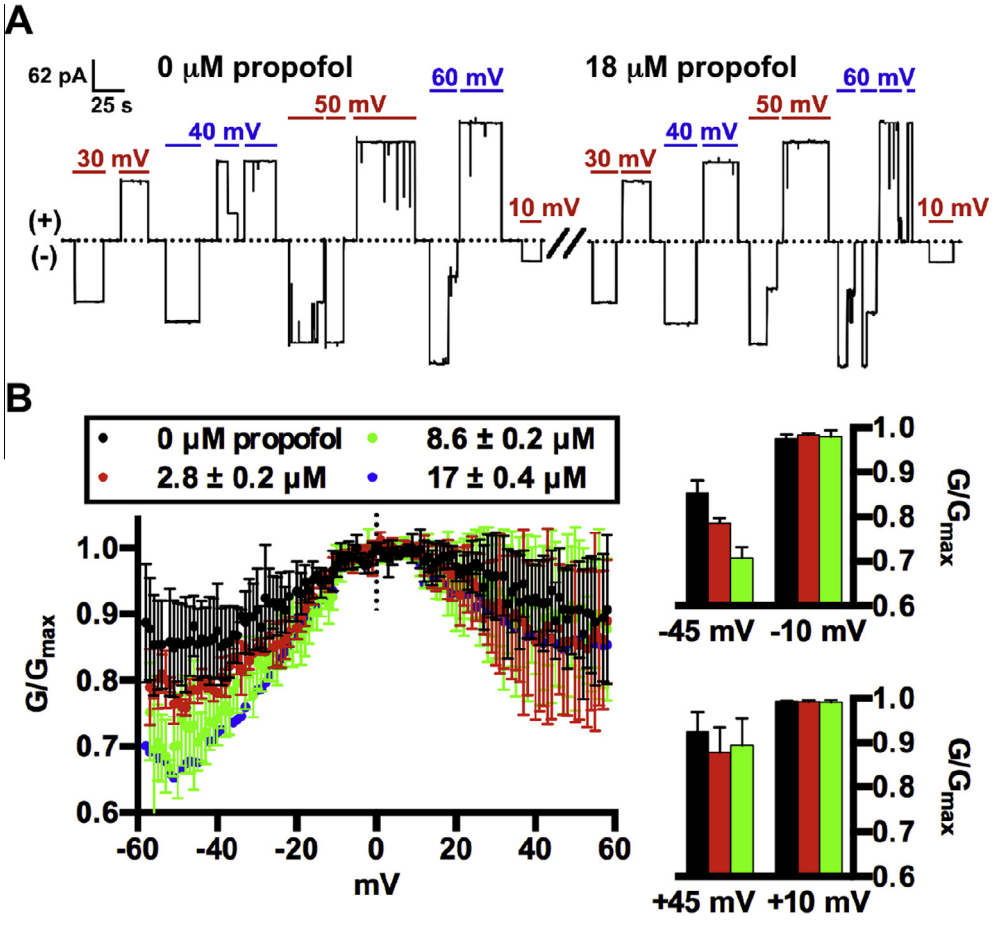

Fig. 2. (A) Current trace from a single VDAC channel reconstituted in a planar bilayer. Negative and positive voltages were alternately applied as indicated. Typical VDAC gating was seen, and the open channel conductance in this experiment was 4.1 nS at each voltage ± propofol. (B) (*Left*), VDAC conductance (G) at each voltage normalized to the maximum conductance for each experiment (G_{max}), which occurs when all channels are open at low voltage. Normalizing by G_{max} accounts for the variable number of channels in the membrane, which ranged between 8 and 22 per experiment. The means ± SD from four (control, 0 μM propofol), three (2.8 and 8.6 μM propofol), or two (17 μM propofol) experiments are shown (SD not shown for 17 μM). (*Right*), the mean G/G_{max} ± SE is shown for select voltages. At −45 mV, G/G_{max} decreased by 8% and 17% with 2.8 and 8.6 μM propofol, respectively, compared to the control.

tionally into these membranes [2], channel gating at positive and negative voltages can be dissociated.

After VDAC closure, and in response to decreasing transmembrane voltage, re-opening of channels is fast (sub-milliseconds) [44], and can be measured as an increase in channel conductance. With a two-state model of VDAC gating, where the channel is either open or closed, the conformational equilibrium of channel re-opening can be quantitatively described by the gating parameters V_0, which is the voltage at which half the channels are open, and n, which is the effective gating charge and describes the steepness of the voltage dependence [2,36]. At negative voltage, propofol did not affect either gating parameters V_0 or n relative to control experiments (Table S3), suggesting that propofol might specifically influence initiation of VDAC gating as opposed to the dynamics associated with channel re-opening.

A similar asymmetric increase in VDAC gating at the same (negative) voltage polarity has been previously observed by increasing the mole fraction of non-lamellar lipids in the membrane [2,45]. This initially suggested that propofol might be affecting VDAC by changing the properties of the surrounding membrane. However, in contrast to propofol, membranes of non-lamellar lipids clearly affect channel re-opening, as the voltage at which half the channels open, V_0, decreases while n remains constant [2]. Non-lamellar lipids likely affect VDAC through increased lipid packing stress on the membrane-embedded channel at the depth of lipid acyl chains. In the proposed model [2], VDAC conformational transitions are sensitive to the pressure in the hydrophobic core of the lipid bilayer, and upon gating at negative voltages, the external shape of the channel can relieve elevated pressures that derive from that depth in the membrane [2,45].

Therefore, to further differentiate the effects of propofol from those of non-lamellar lipids, we performed experiments with gramicidin A, an ion channel with properties known to be modulated by lipid bilayer mechanics. This channel is a sensitive molecular probe of, e.g., lipid packing stress [2,46–48]. Gramicidin A forms shorter-lived channels as the fraction of non-lamellar lipid in the membrane increases [2,48]; however, propofol (1–40 μM) did not affect gramicidin A channel lifetime or conductance in DOPC/DOPE membranes (Fig. S4).

The absence of a propofol effect on gramicidin A suggests that the general anesthetic acts directly on VDAC through protein binding, potentially through our identified sites. The measured effect of propofol is enhanced VDAC closure at negative potentials. Together, the locations of these sites suggest that the distal portions of β-strands regulate the dynamics associated with initiating closure. The physiological role of VDAC gating itself is a matter of conjecture [49], and future work will aim to determine the relevance of enhanced closure. Although it is unlikely that VDAC modulation contributes to anesthetic hypnosis [12], potentiation of gating could potentially modulate neuronal apoptosis or metabolism [49].

Acknowledgements

We thank Tatiana Rostovtseva and Oscar Teijido for their excellent guidance with VDAC electrophysiology techniques, and we thank Michael Weinrich for performing the gramicidin A recordings. This work was partially supported by the Solomon and Catherine Erulkar Traveling Fellowship awarded to B.P.W. Other support was provided by the National Institutes of Health, including through Grants F31-NS080519 and P01-GM055876.

Appendix A. Supplementary data

Supplementary data associated with this article can be found, in the online version, at http://dx.doi.org/10.1016/j.febslet.2014.10.009.

References

[1] Colombini, M., Blachly-Dyson, E. and Forte, M. (1996) VDAC, a channel in the outer mitochondrial membrane. Ion Channels 4, 169–202.
[2] Rostovtseva, T.K., Kazemi, N., Weinrich, M. and Bezrukov, S.M. (2006) Voltage gating of VDAC is regulated by nonlamellar lipids of mitochondrial membranes. J. Biol. Chem. 281, 37496–37506.
[3] Mlayeh, L., Chatkaew, S., Léonetti, M. and Homblé, F. (2010) Modulation of plant mitochondrial VDAC by phytosterols. Biophys. J. 99, 2097–2106.
[4] Bowen, K.A., Tam, K. and Colombini, M. (1985) Evidence for titratable gating charges controlling the voltage dependence of the outer mitochondrial membrane channel, VDAC. J. Membr. Biol. 86, 51–59.
[5] Teijido, O., Rappaport, S.M., Chamberlin, A., Noskov, S.Y., Aguilella, V.M., et al. (2014) Acidification affects voltage-dependent anion channel functioning asymmetrically: role of salt bridges. J. Biol. Chem. 289, 23670–23682.
[6] Gurnev, P.A., Rostovtseva, T.K. and Bezrukov, S.M. (2011) Tubulin-blocked state of VDAC studied by polymer and ATP partitioning. FEBS Lett. 585, 2363–2366.
[7] Bauer, A.J., Gieschler, S., Lemberg, K.M., McDermott, A.E. and Stockwell, B.R. (2011) Functional model of metabolite gating by human voltage-dependent anion channel 2. Biochemistry 50, 3408–3410.
[8] Weiser, B.P., Woll, K.A., Dailey, W.P. and Eckenhoff, R.G. (2014) Mechanisms revealed through general anesthetic photolabeling. Curr. Anesthesiol. Rep. 4, 57–66.
[9] Xi, J., Liu, R., Asbury, G.R., Eckenhoff, M.F. and Eckenhoff, R.G. (2004) Inhalational anesthetic-binding proteins in rat neuronal membranes. J. Biol. Chem. 279, 19628–19633.
[10] Pan, J.Z., Xi, J., Tobias, J.W., Eckenhoff, M.F. and Eckenhoff, R.G. (2007) Halothane binding proteome in human brain cortex. J. Proteome Res. 6, 582–592.
[11] Darbandi-Tonkabon, R., Hastings, W.R., Zeng, C.-M., Akk, G., Manion, B.D., et al. (2003) Photoaffinity labeling with a neuroactive steroid analogue. 6-Azi-pregnanolone labels voltage-dependent anion channel-1 in rat brain. J. Biol. Chem. 278, 13196–13206.
[12] Darbandi-Tonkabon, R., Manion, B.D., Hastings, W.R., Craigen, W.J., Akk, G., et al. (2004) Neuroactive steroid interactions with voltage-dependent anion channels: lack of relationship to GABAA receptor modulation and anesthesia. J. Pharmacol. Exp. Ther. 308, 502–511.
[13] Chen, Z.-W., Manion, B., Townsend, R.R., Reichert, D.E., Covey, D.F., et al. (2012) Neurosteroid analog photolabeling of a site in the third transmembrane domain of the β3 subunit of the GABA(A) receptor. Mol. Pharmacol. 82, 408–419.
[14] Husain, S.S., Forman, S.A., Kloczewiak, M.A., Addona, G.H., Olsen, R.W., et al. (1999) Synthesis and properties of 3-(2-hydroxyethyl)-3-*n*-pentyldiazirine, a photoactivable general anesthetic. J. Med. Chem. 42, 3300–3307.
[15] Pratt, M.B., Husain, S.S., Miller, K.W. and Cohen, J.B. (2000) Identification of sites of incorporation in the nicotinic acetylcholine receptor of a photoactivatible general anesthetic. J. Biol. Chem. 275, 29441–29451.
[16] Husain, S.S., Ziebell, M.R., Ruesch, D., Hong, F., Arevalo, E., et al. (2003) 2-(3-Methyl-3H-diaziren-3-yl)ethyl 1-(1-phenylethyl)-1H-imidazole-5-carboxylate: a derivative of the stereoselective general anesthetic etomidate for photolabeling ligand-gated ion channels. J. Med. Chem. 46, 1257–1265.
[17] Husain, S.S., Nirthanan, S., Ruesch, D., Solt, K., Cheng, Q., et al. (2006) Synthesis of trifluoromethylaryl diazirine and benzophenone derivatives of etomidate that are potent general anesthetics and effective photolabels for probing sites on ligand-gated ion channels. J. Med. Chem. 49, 4818–4825.
[18] Husain, S.S., Stewart, D., Desai, R., Hamouda, A.K., Li, S.G.-D., et al. (2010) *p*-Trifluoromethyldiazirinyl-etomidate: a potent photoreactive general anesthetic derivative of etomidate that is selective for ligand-gated cationic ion channels. J. Med. Chem. 53, 6432–6444.
[19] Ziebell, M.R., Nirthanan, S., Husain, S.S., Miller, K.W. and Cohen, J.B. (2004) Identification of binding sites in the nicotinic acetylcholine receptor for [3H]azietomidate, a photoactivatable general anesthetic. J. Biol. Chem. 279, 17640–17649.
[20] Hamouda, A.K., Stewart, D.S., Husain, S.S. and Cohen, J.B. (2011) Multiple transmembrane binding sites for *p*-trifluoromethyldiazirinyl-etomidate, a photoreactive Torpedo nicotinic acetylcholine receptor allosteric inhibitor. J. Biol. Chem. 286, 20466–20477.
[21] Emerson, D.J., Weiser, B.P., Psonis, J., Liao, Z., Taratula, O., et al. (2013) Direct modulation of microtubule stability contributes to anthracene general anesthesia. J. Am. Chem. Soc. 135, 5389–5398.
[22] Weiser, B.P., Kelz, M.B. and Eckenhoff, R.G. (2013) In vivo activation of azipropofol prolongs anesthesia and reveals synaptic targets. J. Biol. Chem. 288, 1279–1285.
[23] Stewart, D.S., Savechenkov, P.Y., Dostalova, Z., Chiara, D.C., Ge, R., et al. (2011) P-(4-Azipentyl)propofol: a potent photoreactive general anesthetic derivative of propofol. J. Med. Chem. 54, 8124–8135.
[24] Hall, M.A., Xi, J., Lor, C., Dai, S., Pearce, R., et al. (2010) M-Azipropofol (AziPm) a photoactive analogue of the intravenous general anesthetic propofol. J. Med. Chem. 53, 5667–5675.
[25] Sims, N.R. and Anderson, M.F. (2008) Isolation of mitochondria from rat brain using Percoll density gradient centrifugation. Nat. Protoc. 3, 1228–1239.
[26] Kayser, H., Kratzin, H.D., Thinnes, F.P., Götz, H., Schmidt, W.E., et al. (1989) Identification of human porins. II. Characterization and primary structure of a

31-lDa porin from human B lymphocytes (Porin 31HL). Biol. Chem. Hoppe Seyler 370, 1265–1278.
[27] Ujwal, R., Cascio, D., Colletier, J.-P., Faham, S., Zhang, J., et al. (2008) The crystal structure of mouse VDAC1 at 2.3 A resolution reveals mechanistic insights into metabolite gating. Proc. Natl. Acad. Sci. U.S.A. 105, 17742–17747.
[28] Lomize, M.A., Pogozheva, I.D., Joo, H., Mosberg, H.I. and Lomize, A.L. (2012) OPM database and PPM web server: resources for positioning of proteins in membranes. Nucleic Acids Res. 40, D370–D376.
[29] The PyMOL Molecular Graphics System, Version 1.5.0.4, Schrödinger LLC.
[30] Song, J., Midson, C., Blachly-Dyson, E., Forte, M. and Colombini, M. (1998) The topology of VDAC as probed by biotin modification. J. Biol. Chem. 273, 24406–24413.
[31] Colombini, M. (2004) VDAC: the channel at the interface between mitochondria and the cytosol. Mol. Cell. Biochem. 256–257, 107–115.
[32] Colombini, M. (2009) The published 3D structure of the VDAC channel: native or not? Trends Biochem. Sci. 34, 382–389.
[33] Blachly-Dyson, E., Peng, S., Colombini, M. and Forte, M. (1990) Selectivity changes in site-directed mutants of the VDAC ion channel: structural implications. Science 247, 1233–1236.
[34] Palmieri, F. and De Pinto, V. (1989) Purification and properties of the voltage-dependent anion channel of the outer mitochondrial membrane. J. Bioenerg. Biomembr. 21, 417–425.
[35] Colombini, M. (1989) Voltage gating in the mitochondrial channel, VDAC. J. Membr. Biol. 111, 103–111.
[36] Thomas, L., Blachly-Dyson, E., Colombini, M. and Forte, M. (1993) Mapping of residues forming the voltage sensor of the voltage-dependent anion-selective channel. Proc. Natl. Acad. Sci. U.S.A. 90, 5446–5449.
[37] Kerner, J., Lee, K., Tandler, B. and Hoppel, C.L. (2012) VDAC proteomics: post-translation modifications. Biochim. Biophys. Acta BBA Biomembr. 1818, 1520–1525.
[38] Komarov, A.G., Deng, D., Craigen, W.J. and Colombini, M. (2005) New insights into the mechanism of permeation through large channels. Biophys. J. 89, 3950–3959.
[39] Schredelseker, J., Paz, A., López, C.J., Altenbach, C., Leung, C.S., et al. (2014) High resolution structure and double electron-electron resonance of the zebrafish voltage-dependent anion channel 2 reveal an oligomeric population. J. Biol. Chem. 289, 12566–12577.
[40] Amodeo, G.F., Scorciapino, M.A., Messina, A., De Pinto, V. and Ceccarelli, M. (2014) Charged residues distribution modulates selectivity of the open state of human isoforms of the voltage dependent anion-selective channel. PLoS One 9, e103879.
[41] Tomasello, M.F., Guarino, F., Reina, S., Messina, A. and De Pinto, V. (2013) The voltage-dependent anion selective channel 1 (VDAC1) topography in the mitochondrial outer membrane as detected in intact cell. PLoS One 8, e81522.
[42] Hansen, A.H., Sørensen, K.T., Mathieu, R., Serer, A., Duelund, L., et al. (2013) Propofol modulates the lipid phase transition and localizes near the headgroup of membranes. Chem. Phys. Lipids 175–176, 84–91.
[43] Vander Heiden, M.G., Chandel, N.S., Li, X.X., Schumacker, P.T., Colombini, M., et al. (2000) Outer mitochondrial membrane permeability can regulate coupled respiration and cell survival. Proc. Natl. Acad. Sci. U.S.A. 97, 4666–4671.
[44] Colombini, M. (1979) A candidate for the permeability pathway of the outer mitochondrial membrane. Nature 279, 643–645.
[45] Rostovtseva, T.K. and Bezrukov, S.M. (2008) VDAC regulation: role of cytosolic proteins and mitochondrial lipids. J. Bioenerg. Biomembr. 40, 163–170.
[46] Lundbaek, J.A. and Andersen, O.S. (1999) Spring constants for channel-induced lipid bilayer deformations. Estimates using gramicidin channels. Biophys. J. 76, 889–895.
[47] Suchyna, T.M., Tape, S.E., Koeppe, R.E., Andersen, O.S., Sachs, F., et al. (2004) Bilayer-dependent inhibition of mechanosensitive channels by neuroactive peptide enantiomers. Nature 430, 235–240.
[48] Weinrich, M., Rostovtseva, T.K. and Bezrukov, S.M. (2009) Lipid-dependent effects of halothane on gramicidin channel kinetics: a new role for lipid packing stress. Biochemistry 48, 5501–5503.
[49] Lemasters, J.J. and Holmuhamedov, E. (2006) Voltage-dependent anion channel (VDAC) as mitochondrial governator—thinking outside the box. Biochim. Biophys. Acta BBA Mol. Basis Dis. 1762, 181–190.